Journal of Fluorine Chemistry 141 (2012) 21–28

Contents lists available at SciVerse ScienceDirect

Journal of Fluorine Chemistry

journal homepage: www.elsevier.com/locate/fluor

Novel anionic fluorine-containing amphiphilic self-assembly polymer micelles for potential application in protein drug carrier

Guoqiang Liu [a], Wen Fan [a], Ling Li [a], Paul K. Chu [b], Kelvin W.K. Yeung [c], Shuilin Wu [a,b,c], Zushun Xu [a,b,c,*]

[a] Ministry-of-Education Key Laboratory for the Green Preparation and Application of Functional Materials, Hubei University, Wuhan 430062, China
[b] Department of Physics & Materials Science, City University of Hong Kong, Tat Chee Avenue, Kowloon, Hong Kong, China
[c] Division of Spine Surgery, Department of Orthopaedics and Traumatology, The University of Hong Kong, Pokfulam, Hong Kong, China

ARTICLE INFO

Article history:
Received 10 February 2012
Received in revised form 18 May 2012
Accepted 23 May 2012
Available online 31 May 2012

Keywords:
Amphiphilic graft copolymer
Self-assembly
Micelle
Anionic
Fluoropolymer
Protein drug carrier

ABSTRACT

A novel series of anionic fluorine-containing amphiphilic graft copolymers, poly(hexafluorobutyl methacrylate-*co*-sodium 4-vinylbenzenesulfonate)-*g*-poly(ethylene glycol) methyl ether methacrylate [poly(HFMA-*co*-NaSS)-*g*-PEG], were prepared *via* the free radical copolymerization. The micellization behavior of the copolymers was studied by critical micelle concentration (CMC), dynamic light scattering (DLS) and transmission electron microscopy (TEM). The results showed that poly(HFMA-*co*-NaSS)-*g*-PEG copolymers could self-assemble into core/shell structure micelles in aqueous solution. Afterward, the micelles stability was studied by zeta potential measurement, which demonstrated that the copolymer micelles had good stability in biological milieu. The interaction between the copolymer micelles and BSA was characterized by fluorescence spectroscopy, and the morphology of the micelles/BSA complexes was observed by TEM. The results demonstrated that the adsorption could be easily achieved between the copolymer micelles and BSA. Furthermore, the cytotoxicity was evaluated *via* MTT viability assay, indicating that the copolymer had low toxicity. Our study suggests that poly(HFMA-*co*-NaSS)-*g*-PEG micelles have a potential application as the protein drug carrier.

1. Introduction

Recently, the scientific and technological interest is increasingly focusing on the development of novel amphiphilic graft copolymers [1–4]. In most cases, the different segments are incompatible giving rise to a rich variety of well-defined self-assembled structures in selective solvents. In aqueous solution, the amphiphilic graft copolymers usually self-assemble to form micelles, in which the water-insoluble core is constituted by the hydrophobic segments, while the hydrophilic segments decorate the core, forming a protective hydrophilic shell. Such features make amphiphilic graft copolymers have a wide range of potential applications, such as pharmaceuticals, cosmetics, paints, coatings, drug delivery and others. Therefore, design and preparation of novel high-performance amphiphilic graft copolymers have attracted much attention [5–7].

Owing to the unique characteristics of fluoropolymers such as high hydrophobicity, high thermal and mechanical stability, gas-dissolving capacity, high fluidity, low dielectric constants, oil- and water-repellency, and very interesting surface properties [8–10], much attention has recently been paid to amphiphilic copolymers with fluorocarbon–hydrocarbon hybrid architectures. Besides, fluorinated polymers have been studied from in the field of biomedical applications, for instance, blood substitutes, gas carriers, bioconversion, extraction, and so forth and cannot be achieved by non-fluorinated amphiphilic copolymers [11,12]. On the one hand, the fluorine-containing amphiphilic copolymers have a strong tendency to self-aggregate into stable, well-organized micelles. On the other hand, these micelles may have unique advantages in drug delivery because they can transmit both hydrophobic molecules and fluorophilic molecules at the same time to the target sites due to the hydrophobic interaction and fluorophilic effect [13–16].

Poly(ethylene glycol) (PEG) is widely used as the hydrophilic side chains in amphiphilic graft copolymers. It is a low cost commercial product that possesses some unique and outstanding properties such as hydrophilicity, biocompatibility, nontoxicity, lack of immunogenicity, metal complexing ability, as well as solubility in water and organic solvents [17–19]. Because the presence of PEG on the surface of protein vectors can enhance biocompatibility, reduce cytotoxicity, and protect drugs from degradation, the amphiphilic graft copolymers with PEG as the side chains have been widely applied in the drug delivery systems [20,21].

* Corresponding author at: Ministry-of-Education Key Laboratory for the Green Preparation and Application of Functional Materials, Hubei University, Wuhan 430062, China. Tel.: +86 27 61120608; fax: +86 27 88665610.
E-mail addresses: zushunxu@hubu.edu.cn, waitingll@yahoo.com (Z. Xu).

0022-1139/$ – see front matter. Crown Copyright © 2012 Published by Elsevier B.V. All rights reserved.
http://dx.doi.org/10.1016/j.jfluchem.2012.05.021

Sodium 4-vinylbenzenesulfonate (NaSS) is an anionic functional monomer, which has been widely employed to prepare the charged polymers. If the amphiphilic copolymers contain negatively charged groups, not only will the micelles be dispersed better to reduce the agglomeration due to the electrostatic repulsion, but also the micelles will have an electrostatic absorption effect on the charged biological macromolecules [22–24]. Thus, the negatively charged amphiphilic copolymers may have potential applications as the protein drug carrier.

Bovine serum albumin (BSA) is often chosen as one model protein drug due to its medical importance, low cost, ready availability, and ligand-binding properties [25–27]. The amphiphilic copolymers micelles as the BSA carrier have been widely studied [28–30], but there has been no report about anionic fluorine-containing amphiphilic graft copolymer micelles for the absorption of BSA.

In this work, a novel series of anionic fluorine-containing amphiphilic graft copolymers poly(HFMA-*co*-NaSS)-*g*-PEG were prepared *via* the free radical copolymerization. Our study suggests that poly(HFMA-*co*-NaSS)-*g*-PEG micelles have a potential application as the protein drug carrier. Importantly, our work is promising for future *in vitro* studies involving the design of novel polymer carriers for protein drugs.

2. Results and discussion

2.1. The composition of poly(HFMA-co-NaSS)-g-PEG graft copolymers

The graft copolymers were prepared *via* the free radical copolymerization of HFMA, PEGMA, and NaSS in MeOH. The chemical structure and molecular weight of the graft copolymers were characterized by FTIR, ^{1}H NMR, ^{19}F NMR and GPC.

2.1.1. FTIR

The FTIR spectrum of poly(HFMA-*co*-NaSS)-*g*-PEG is displayed in Fig. 1. The stretching vibration absorption peak of ether linkage appears at 1104 cm^{-1}. The peak at 1737 cm^{-1} is attributed to the characteristic stretching absorption of C=O. Those peaks at 2952 cm^{-1}, 1600–1450 cm^{-1} and 839 cm^{-1} are attributed to the characteristic absorption of the substituting benzene ring. The characteristic absorption peak of S=O bond in NaSS is observed at 1247 cm^{-1}. The peaks at 1000–1260 cm^{-1} are wider and blunter because of the overlap between the stretching vibration absorption of the C–F bond at 1100–1260 cm^{-1} and the stretching vibration absorption of the C–O–C bond at 1250 cm^{-1}. These results reveal that HFMA, NaSS and PEGMA all participate in the polymerization.

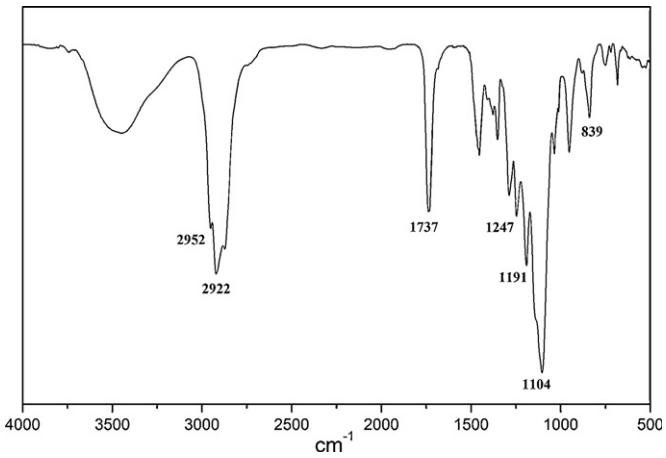

Fig. 1. FTIR spectra of poly(HFMA-*co*-NaSS)-*g*-PEG.

2.1.2. ^{1}H NMR

The ^{1}H NMR spectrum of poly(HFMA-*co*-NaSS)-*g*-PEG is shown in Fig. 2. The characteristic double peaks at 7.76 ppm (h) and 7.05 ppm (h) are attributed to –CH– of benzene ring, the peak at 5.00 ppm (g) is assigned to –CHFCF$_3$, the peak at 4.11 ppm (f) is assigned to –OCH$_2$–CF$_2$–, the peaks at 3.54 ppm (d) and 3.34 ppm (e) are attributable to the methylene protons and terminal methoxy protons of PEG, the peak at 2.45 ppm (i) is assigned to

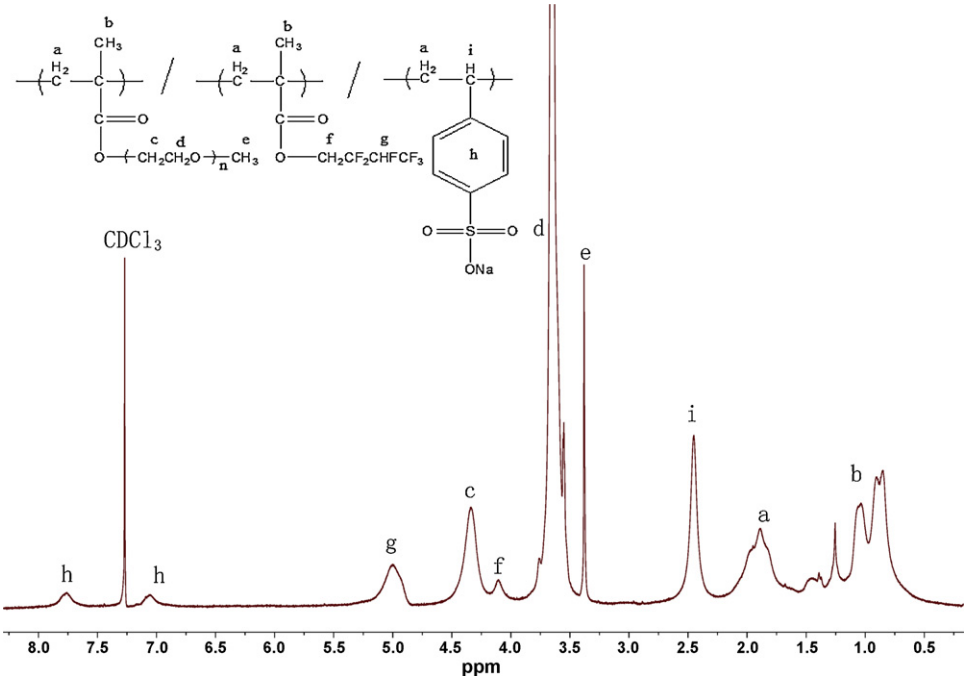

Fig. 2. ^{1}H NMR spectra of poly(HFMA-*co*-NaSS)-*g*-PEG.

Table 1
Recipe, conversion and characteristic data of the graft copolymers.

Sample code	HFMA (g)	PEGMA (g)	NaSS (g)	Conversion (%)	HFMA (wt%)[a]	NaSS (wt%)[a]	$M_n \times 10^4$ (M_w/M_n)[b]	CMC (mg/mL)[c]	Diameter (nm) (PDI)[d]
PEG–F25Na5	0.511	1.427	0.108	95.8	24.2	5.31	3.71 (1.25)	0.235	164 (0.094)
PEG–F35Na5	0.698	1.214	0.101	96.2	36.7	4.87	3.40 (1.19)	0.213	151 (0.088)
PEG–F45Na5	0.902	1.006	0.100	94.3	43.2	5.22	3.18 (1.27)	0.179	136 (0.132)
PEG–F55Na5	1.103	0.802	0.105	95.7	56.8	4.93	2.86 (1.21)	0.166	121 (0.069)
PEG–F65Na5	1.302	0.603	0.103	94.6	64.3	4.81	2.17 (1.32)	0.150	103 (0.114)
PEG–F45Na1	0.909	1.085	0.021	96.6	43.7	0.98	3.26 (1.17)	0.172	117 (0.096)
PEG–F45Na3	0.903	1.047	0.065	94.8	45.2	3.13	3.19 (1.33)	0.176	136 (0.142)
PEG–F45Na7	0.908	0.970	0.144	95.6	44.3	6.58	3.15 (1.25)	0.183	142 (0.083)
PEG–F45Na9	0.902	0.936	0.181	95.9	43.6	10.21	3.03 (1.22)	0.188	147 (0.065)

[a] NMR results.
[b] GPC results.
[c] Surface tension measurement results.
[d] DLS measurement results.

–CH– of the main chains, the peak at 1.89 ppm (a) is assigned to –CH_2– of the main chains, the signals due to terminal methyl group protons of HFMA and PEGMA are seen at 0.80–1.45 ppm (b).

The HFMA and NaSS contents in the graft copolymers were calculated by the ^{1}H NMR peak intensity ratios of the –OCH_2–CF_2– (δ = 4.11 ppm) protons of HFMA, –CH– protons (δ = 7.76 ppm and 7.05 ppm) in the benzene ring of NaSS and the CH_3O-proton (δ = 3.34 ppm) of PEGMA. Table 1 summarizes the HFMA and NaSS contents in each graft copolymer.

2.1.3. ^{19}F NMR

As shown in Fig. 3, the ^{19}F NMR spectrum of the graft copolymers confirms the presence of three different kinds of fluorine resonances originating from HFMA. The peak at −75.3 ppm is assigned to the end –CF_3 group and that at −213.0 ppm to the –CHF_2 group. Because of the influence of the neighboring asymmetric center, the peak of –OCH_2CF_2– splits into two peaks at −114.4 ppm and −120.3 ppm.

2.1.4. GPC

The molecular weight and molecular weight distribution of the copolymers are determined by GPC. The measurement data is listed in Table 1. The results indicate that the copolymerization was successfully carried out, obtaining the high molecular weight and unimodal molecular weight distribution copolymers.

2.2. CMC determination

The amphiphilic graft copolymers can aggregate to form micelles above the critical micelle concentration (CMC). The surface tension measurement over a wide range of concentrations is often used in the CMC determination.

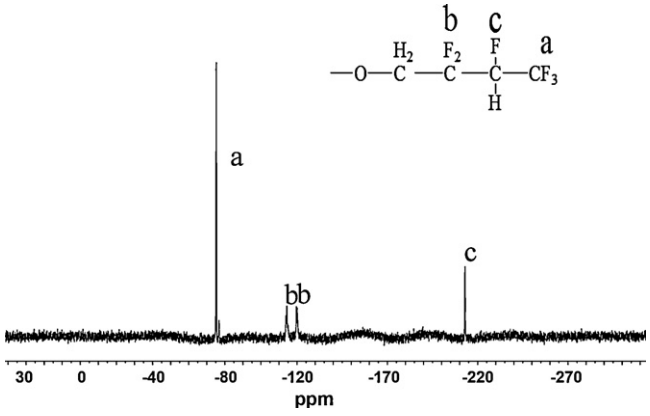

Fig. 3. ^{19}F NMR spectrum of poly(HFMA-*co*-NaSS)-*g*-PEG.

Fig. 4 shows the surface tension *versus* concentration plots of PEG–F45Na5 and PEG–F65Na5. It is clear from the plot of PEG–F45Na5 that there is an inflection point at the characteristic concentration of 0.179 mg/mL. The results demonstrate that PEG–F45Na5 copolymers can form micelles in aqueous solution, and the critical micelle concentration at 25 °C is 0.179 mg/mL. With regard to PEG–F65Na5, the inflection point appears at the concentration of 0.150 mg/mL, indicating that PEG–F65Na5 copolymers also form micelles in aqueous solution and the CMC at 25 °C is 0.150 mg/mL. The CMC values of the nine samples are listed in Table 1.

As shown in Table 1, with increasing the HFMA segment in the copolymers, the CMC decreases gradually, which indicates that the fluorinated segment enhances the surface activity of the amphiphilic copolymer poly(HFMA-*co*-NaSS)-*g*-PEG. The experimental results are in good agreement with those previously reported [31]. On the contrary, the increasing NaSS segment leads to an increase in the CMC of poly(HFMA-co-NaSS)-g-PEG. It may be explained by that the hydrophilic PNaSS segment enhances the hydrophilicity of the fluorine-containing graft copolymers.

2.3. Dynamic light scattering

To investigate the size of the copolymer micelles, dynamic light scattering (DLS) technique is employed to measure the average hydrodynamic diameter and size distribution in aqueous solution. Fig. 5(A) shows the average hydrodynamic diameter and size distribution of different types of copolymer micelles with the same concentration (0.50 mg/mL).

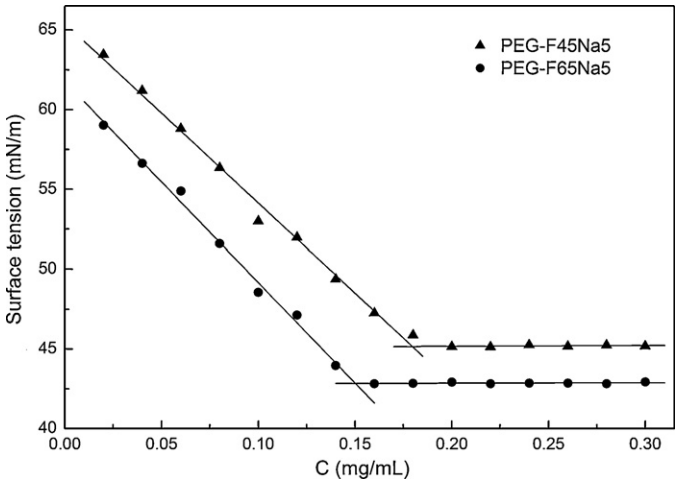

Fig. 4. Surface tension *versus* concentration plots of PEG–F45Na5 and PEG–F65Na5 at 25 °C.

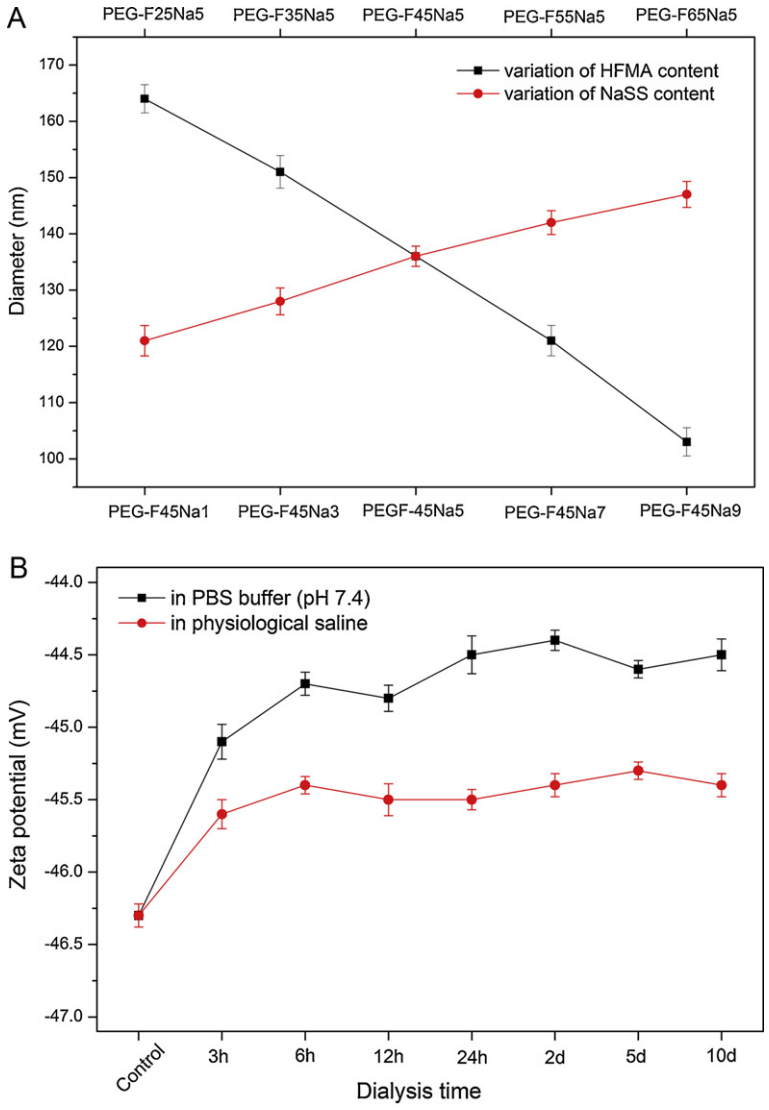

Fig. 5. (A) Hydrodynamic diameters and distribution of different types of the copolymer micelles (the concentrations were all kept at 0.50 mg/mL). (B) The variation of zeta potential of PEG–F45Na5 micelles after different dialysis time periods in phosphate buffer solutions (pH 7.4) and physiological saline, respectively.

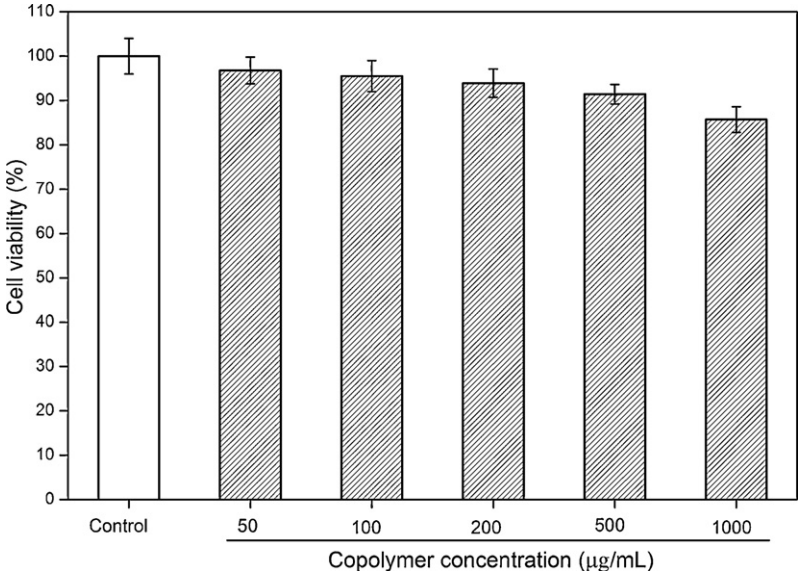

Fig. 6. Caco-2 cell viability treated with different concentrations of PEG–F45Na5 solutions.

As shown in Fig. 5(A) and Table 1, poly(HFMA-*co*-NaSS)-*g*-PEG graft copolymers form nanometer-sized micelles with a narrow particle size distribution in aqueous solution. As the HFMA content of the copolymer increases, the diameter of micelles decreases gradually. This may be attributed to the strong hydrophobicity of the fluorinated segment. In aqueous solution, the hydrophilic PEG chains exist in the stretched state, while the fluorinated chains exist in the state of shrinkage. Thus, the copolymers comprising more HFMA content tend to form smaller micelles. On the contrary, with increasing the NaSS content of the copolymer, the diameter of micelles increases gradually. Due to the negatively charged sulfonic groups (SO_3^-), there is electrostatic repulsion in the micelles. Thus, the increase in the content of NaSS results in the enlargement of electrostatic repulsion, which subsequently leads to an increase in the micelle size.

2.4. The micelle stability

The stability in biological milieu is an important factor when choosing an appropriate protein drug carrier, so the zeta potential of PEG–F45Na5 micelles is measured to investigate the stability of the copolymer micelles under the physiological pH and salt presences. Fig. 5(B) shows the variation of zeta potential of micelles after different dialysis time periods in phosphate buffer solutions (pH 7.4) or physiological saline (NaCl aqueous solutions, 0.154 mol/L), respectively.

As shown in Fig. 5(B), the zeta potential of the micelles in ultrapure water is −46.3 mV. When the micelles are dialyzed against PBS buffer or physiological saline, the initial negative zeta potential increases slightly. This may be caused by the electrostatic shielding effect of salt solution. However, after later dialysis time periods, the zeta potential has no obvious change both in PBS buffer and in physiological saline. These results demonstrate that the PEG–F45Na5 micelles have good stability in biological milieu, which provide a requirement for the micelles as the drug carrier.

2.5. In vitro cytotoxicity

It is well known that the cytotoxicity of biomaterials is extremely important for their applications in drug delivery system. Based on the similarity of the molecular structure, the *in vitro* cytotoxicity of PEG–F45Na5 micelles is evaluated referenced to Caco-2 colon cancer cells using the MTT assay. Fig. 6 displays the cell viability after 48 h incubation in the copolymer solutions with different concentrations. The data demonstrates the micelles do not show obvious cytotoxicity against Caco-2 cells. About 87% of cells are still viable even at a high concentration of 1000 μg/mL. The results indicate that PEG–F45Na5 copolymers have good cytocompatibility.

2.6. Fluorescence spectroscopy

To study the interaction between BSA and poly(HFMA-*co*-NaSS)-*g*-PEG, the fluorescence spectroscopy technique was used to measure the emission spectra of BSA in copolymer solutions. BSA can fluoresce when excited by UV light because of the existence of tryptophan residues. Specifically, the strongest characteristic fluorescence emission peak is at 348 nm with the excitation wavelength of 280 nm. When foreign substances interact with BSA, the property of the characteristic peak will change [12]. Thus, the fluorescence spectroscopy can be employed to investigate the interaction between poly(HFMA-*co*-NaSS)-*g*-PEG and BSA.

Fig. 7(A) shows the fluorescence spectra of BSA in PEG–F45Na5 solutions at different concentrations. It is clear that when PEG–F45Na5 is added, the fluorescence intensity of BSA at 348 nm decreases. Importantly, the emission peak exhibits an obvious blue shift (toward lower wavelength). These results reveal the strong interaction between PEG–F45Na5 and BSA. Besides, with increasing the concentration of PEG–F45Na5 solution, the fluorescence intensity decreases gradually. Compared with the fluorescence intensity below the CMC (0.179 mg/mL), the degree of the decrease is more significant above the CMC. Below the CMC, there is an electrostatic interaction between the negatively charged copolymers and BSA. But above the CMC, PEG–F45Na5 copolymers self-assemble

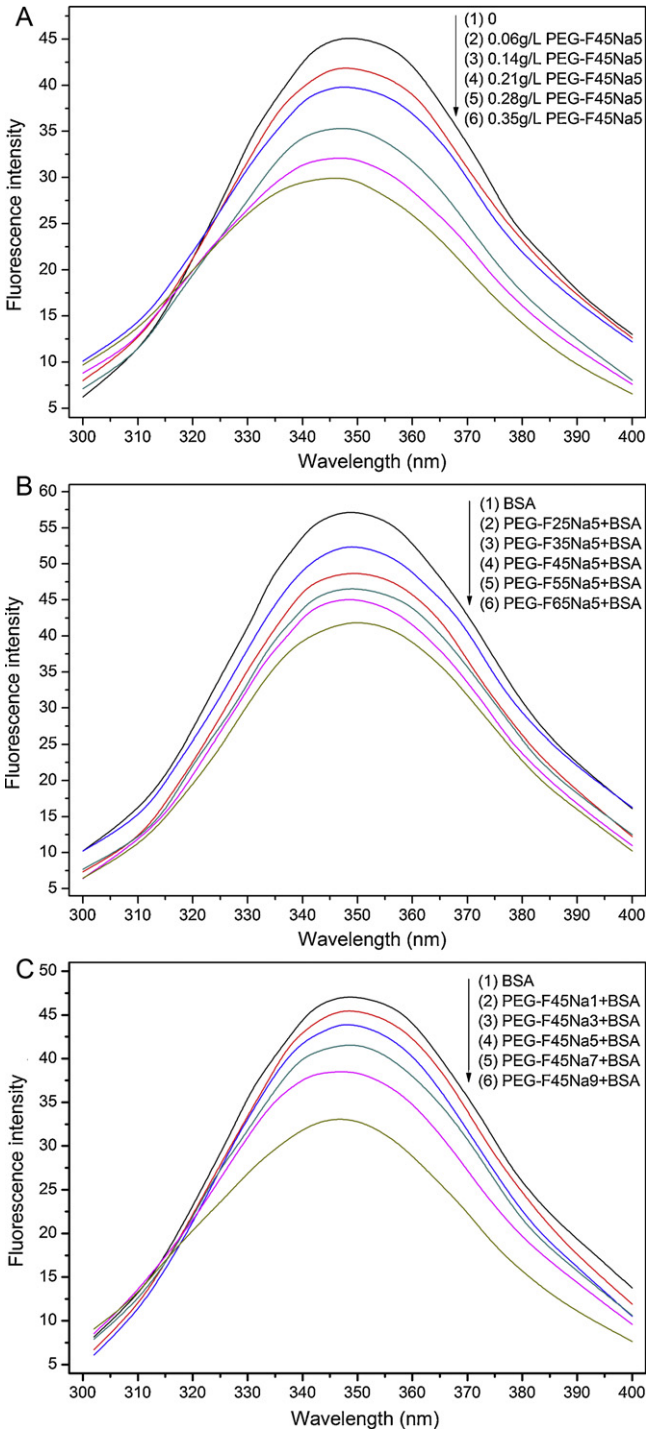

Fig. 7. (A) Fluorescence spectra of BSA in different concentrations of PEG–F45Na5 solutions, (B) fluorescence spectra of BSA in different types of PEG–FXNa5 solutions (all the PEG–FXNa5 concentrations were kept at 0.50 mg/mL), (C) fluorescence spectra of BSA in different types of PEG–F45NaY solutions all the PEG–F45NaY concentrations were kept at 0.50 mg/mL). BSA concentration was kept at 0.68 mg/mL and the volume ratio of PEG–FXNaY:BSA was 5:1.

to form micelles, and the hydrophobic fluorinated segment gathers in the interior of the micelles. Because of tryptophan, tyrosine, phenylalanine and other hydrophobic groups in the BSA molecules, there is a hydrophobic interaction between BSA and PEG–F45Na5 micelles. Therefore, when the concentration of PEG–F45Na5 solution is above the CMC, in addition to electrostatic interaction, there is a strong hydrophobic interaction. With increasing the concentration of the graft copolymers, both hydrophobic interaction and electrostatic interaction become stronger, which enhances the energy loss of collision, non-radiative deactivation process and other quenching effects. Hence, the fluorescence yield of BSA molecules decreases and the fluorescence intensity decreases gradually.

Fig. 7(B) displays the fluorescence spectra of BSA in different types of PEG–FXNa5 solutions (0.50 mg/mL, above the CMC). As the content of HFMA in the PEG–FXNa5 increases, the fluorescence intensity of BSA decreases gradually and the emission peak still does not exhibit blue shift. It may be explained by that the increasing fluorinated segment in the copolymers leads to an increase in the hydrophobic interaction between PEG–FXNa5 micelles and BSA, specifically, the hydrophobic interaction have not cause the blue shift of the emission peak.

Fig. 7(C) exhibits the fluorescence spectra of BSA in different types of PEG–F45NaY solutions (0.50 mg/mL, above the CMC). As the content of NaSS in the PEG–F45NaY micelles increases, the fluorescence intensity of BSA decreases gradually, and the blue shift of the emission peak becomes more and more remarked. The results demonstrate that the increasing negatively charged segment in the copolymers leads to an increase in the electrostatic interaction between PEG–F45NaY micelles and BSA, and the electrostatic interaction not only lowers the fluorescence intensity of BSA, but also enhances the blue shift of the emission peak. It is noteworthy that the electrostatic interaction can affect the arrangement of positive and negative charges in the BSA molecules, leading to the slight change of the spatial structure of BSA molecules, so the blue shift occurs.

The fluorescence results reveal that there are both electrostatic interaction and hydrophobic interaction between poly(HFMA-*co*-NaSS)-*g*-PEG micelles and BSA. Both interactions contribute to the decrease in the fluorescence intensity of BSA, but only electrostatic interaction causes the blue shift of the emission peak, which may be attributed to the increase of electron density in the self-assembly polymer micelles [32,33].

2.7. TEM measurement

To study the morphology of poly(HFMA-*co*-NaSS)-*g*-PEG micelles and BSA absorption on the micelles, transmission electron microscopy was employed to observe PEG–F45Na5 micelles, pure BSA, and PEG–F45Na5 micelles/BSA complex. Fig. 8(A–C) exhibits TEM images of PEG–F45Na5 micelles, pure BSA, and PEG–F45Na5 micelles/BSA complexes.

As shown in Fig. 8(A), in aqueous solution, the PEG–F45Na5 copolymers form spherical micelles with a core/shell structure, whose diameter is about 130 nm. Due to the hydrophobic characteristic of the fluorinated chains in the copolymers, during the self-assembly process, they have a high tendency to bury themselves in the interior of the micelles and form a highly hydrophobic core. On the contrary, the hydrophilic PEG chains and NaSS segment form the shell of micelles.

Fig. 8(B) shows the image of pure BSA, which has a crystalline structure in aqueous solution. Fig. 8(C) displays the image of PEG–F45Na5 micelles/BSA complexes in aqueous solution. When BSA is added into the PEG–F45Na5 micelles solution, the obtained aggregates are still relatively regular spherical micelles, but the crystalline structures disappear. Compared with the micelles in Fig. 8(A), the particle size increases significantly, and the aggregates change from a core/shell structure into a hollow-like one. Due to electrostatic interaction and hydrophobic interaction between BSA and poly(HFMA-*co*-NaSS)-*g*-PEG micelles, BSA molecules migrate from the aqueous phase to the micellar phase combining with the copolymer chains. As the water evaporates, the chain entanglement between PEG–F45Na5 and BSA gets tighter, and the nuclear phase of micelles collapses to the inner surface of the shell. Therefore, the PEG–F45NaSS micelles/BSA complexes form the hollow-like structure.

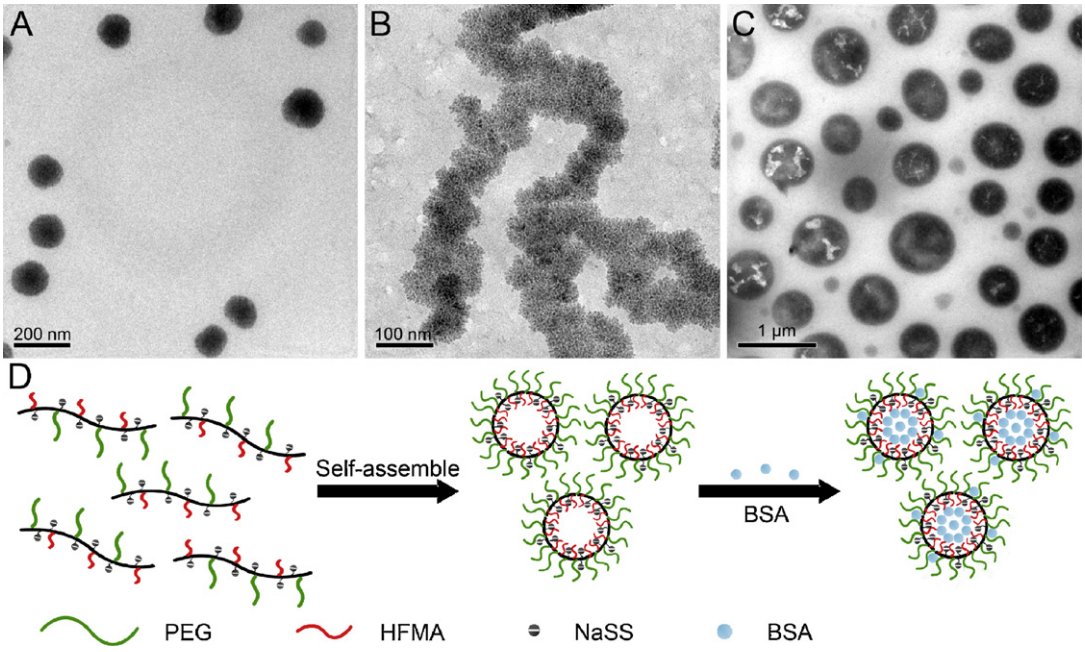

Fig. 8. TEM images of (A) PEG–F45Na5 micelles in aqueous solution (0.50 mg/mL), (B) pure BSA in aqueous solution (0.68 mg/mL), and (C) PEG–F45Na5 micelles/BSA complexes (PEG–F45Na5 concentration was kept at 0.50 mg/mL, BSA concentration was kept at 0.68 mg/mL, volume ratio of PEG–F45Na5:BSA was 5:1), (D) schematic diagram illustrating the formation of self-assembled micelles and the process of loading BSA.

TEM results show that poly(HFMA-*co*-NaSS)-*g*-PEG micelles can self-assemble into core/shell structure micelles in aqueous solution and have a significant absorption effect on BSA. Fig. 8(D) illustrates the formation of the self-assembled micelles and the process of loading BSA.

3. Conclusions

We have successfully prepared a series of novel anionic fluorine-containing amphiphilic graft copolymers poly(HFMA-*co*-NaSS)-*g*-PEG. Well-defined characterization for the copolymers was performed through FTIR, ^{1}H NMR, ^{19}F NMR, and GPC. The graft copolymers could self-assemble into core/shell structure micelles in aqueous solution. The copolymer micelles had good stability and low toxicity in biological milieu. Fluorescence spectroscopy revealed electrostatic and hydrophobic interaction between the micelles and BSA, and TEM images showed that the micelles had a significant absorption effect on BSA. Our study suggests that poly(HFMA-*co*-NaSS)-*g*-PEG micelles have a potential application as the protein drug carrier.

4. Experimental

4.1. Materials

2,2,3,4,4,4-Hexafluorobutyl methacrylate (HFMA) was purchased from Xeogia Fluorine-Silicon Chemical Company (Harbin, China, chemical purity), and was distilled under reduced pressure before use. Poly(ethylene glycol) methyl ether methacrylate (PEGMA) (average molecular weight of 1100 g/mol) and sodium 4-vinylbenzenesulfonate (NaSS) was obtained from Aldrich, purified by vacuum-drying at room temperature for 24 h before use. Methanol (MeOH) purchased from Shanghai Chemical Reagents Co. (Shanghai, China, chemical purity) serving as solvent was distilled under reduced pressure before use. Tetrahydrofuran (THF) purchased from Shanghai Chemical Reagents Co. (Shanghai, China, chemical purity) serving as extracting agent was initially dried over potassium hydroxide at least overnight and then refluxed over sodium wire for 3 days before use. Bovine serum albumin (BSA, average molecular weight of 68,000 g/mol) was supplied by Beijing Shuangxuan Biological Culture Medium Plant (Beijing, China). The human colonic carcinoma cell line Caco-2 was obtained from the American Type Culture Collection (ATCC HTB 37). Analytical grade 2,2-azobisisobutyronitrile (AIBN) was purified by recrystallization in ethanol. All the other chemicals were analytical grade and used without further purification. Ultrapure water was used in all the preparation and characterization processes.

4.2. Preparation of poly(HFMA-co-NaSS)-g-PEG graft copolymers

The graft copolymers were prepared *via* conventional free radical polymerization in MeOH. In a typical reaction, PEGMA macromonomer (0.605 g, 0.550 mmol), HFMA (1.302 g, 5.205 mmol), NaSS (0.102 g, 0.495 mmol), AIBN (0.012 g 0.073 mmol), and MeOH (15 mL) were added into a 25 mL round bottom flask containing a magnetic stirrer. The flask was then deoxygenated under reduced pressure and backfilled with nitrogen several times. Polymerization was carried out at 75 °C for 24 h. The product was isolated by evaporating the solvent to dryness in a rotary evaporator and then the mixture was precipitated in n-hexane. After filtration, the precipitate was purified by re-precipitation repeatedly in n-hexane. The obtained product was dried under vacuum at 30 °C for 48 h. Polymerization conversion was determined by gravimetric analysis. The product was analyzed by FTIR, ^{1}H NMR, and ^{19}F NMR, and GPC. The detailed polymerization conditions are listed in Table 1. Here, the abbreviation scheme PEG–F*X*Na*Y* is used, where *X* represents the theoretical HFMA wt% in the graft copolymer and *Y* represents the theoretical NaSS wt% in the graft copolymer. Hence, for example, PEG–F45Na5 is a graft copolymer with 45 wt% of HFMA content and 5 wt% of NaSS content.

4.3. Preparation of the copolymer micelle solution

The dialysis technique was employed to prepare the micelle solution. The graft copolymers were dissolved in a small amount of THF. The copolymers/THF solution was filtered through a Millipore filter with 450 nm pore size, and then added into a certain amount of ultrapure water. Afterward, the mixture was placed into a dialysis bag (Molecular weight Cut Off (MWCO) = 8000–14,000) and dialyzed against 1000 mL ultrapure water (water changed every 6 h) for 3 days to remove THF. After these processes, the copolymer micelle solution was obtained.

4.4. FTIR characterization

FTIR spectra were performed on the Perkin-Elmer Spectrum one Transform Infrared Spectrometer (Perkin-Elmer, USA). The polymer films were cast onto KBr disks from THF solution. The FTIR spectra were recorded from 4000 to 500 cm^{-1}.

4.5. ^{1}H NMR and ^{19}F NMR characterization

^{1}H NMR and ^{19}F NMR spectra were recorded using a UNITY INVOA-600 MHz spectrometer (Varian, USA) at 20 °C.

4.6. GPC characterization

The molecular weight and molecular weight distribution of the copolymers were determined by a Waters 150-C gel permeation chromatograph (GPC) at 25 °C. THF was used as the eluent at a flow rate of 1.0 mL/min, and polystyrene standards were used for calibration.

4.7. Surface tension measurement

The surface tension measurement was carried out by the pendant drop method using a Krŭss interface tension meter (KrŭssGmbH, Hamburg, Germany) at 25 °C. The aqueous solutions of the copolymers were prepared by dissolving the pure copolymers in ultrapure water.

4.8. Dynamic light scattering

The average hydrodynamic radius and size distribution of the micelles were measured by dynamic light scattering (DLS) (Autosize Loc-Fc-963, Malvern Instrument). Measurements were carried out at an angle of 90° with 679 nm wavelength laser light at 25 °C. Sample cell was thermostated for 5 min prior to measurement.

4.9. Zeta potential measurement

The micelle stability in biological milieu was studied by measuring the variation of zeta potential. The PEG–F45Na5 micelle solution (0.50 mg/mL) was dialyzed against 1000 mL phosphate buffer solutions (pH 7.4) or physiological saline (NaCl aqueous solution, 0.154 mol/L), respectively. The zeta potential was determined by Malvern Zetasizer Nano ZS (Malvern Instruments, Malvern, UK) after different dialysis time periods.

4.10. In vitro cytotoxicity

In vitro cytotoxicity of the graft copolymers was measured by an MTT viability assay against Caco-2 cells. The cells were seeded at a

density of 1×10^4 cells/well in 96-well plates in a standard growth medium at 37 °C for 24 h. Then the culture medium was removed and the copolymer solution was added into the plates at different concentrations. Meanwhile, the wells containing only the cell medium were also prepared as untreated controls. After the cells were incubated for another 48 h, the medium was removed and 20 μL MTT solutions (5 mg/mL) were added into each well. Then the cells were incubated for an additional 4 h. The supernatant was discarded, followed by addition of DMSO (150 μL/well) and agitation for 30 s to completely dissolve the crystals. The absorbance of each well was measured at a wavelength of 570 nm by a microplate reader, and the cell viability was calculated by the following formula:

Cell viability (%) = OD_{570}(sample)/OD_{570}(control) × 100, where OD_{570}(sample) is the optical density (OD) of the treated cells and OD_{570}(control) represents that of the untreated control cells.

4.11. Fluorescence spectroscopy

The fluorescence properties of copolymers/BSA mixtures were studied on a RF-540 (Hitachi High-technologies Corp., Tokyo, Japan) spectrometer. The concentration of BSA aqueous solution was 0.68 mg/mL. The fluorescence emission spectra were recorded in the wavelength range 300–400 nm with the fixed excitation wavelength of 280 nm.

4.12. Transmission electron microscopy

The morphology of the micelles, pure BSA and copolymers/BSA complexes were characterized by TEM (Tecnai G20, FEI Corp., USA). A drop of the sample was placed on a Formvar-coated copper grid, and then dried in air. The TEM images were obtained at 25 °C at an electron acceleration voltage of 200 kV.

Acknowledgments

The work was supported by the Key Projects in the National Science & Technology Pillar Program during the Eleventh Five-year Plan Period (No. 2008BAC32B03) and the National Natural Science Foundation of China (No. 50973027).

References

[1] X. Luo, G. Wang, X. Pang, J. Huang, Macromolecules 41 (2008) 2315–2317.
[2] N.A. Hashim, F. Liu, K. Li, Journal of Membrane Science 345 (2009) 134–141.
[3] X. Qiu, C. Wang, J. Shen, M. Jiang, Carbohydrate Polymers 83 (2011) 1723–1729.
[4] C.S. Chem, W.Y. Chen, H.C. Chiu, F.H. Chang, M.H. Hsieh, J.R. Tu, Colloids and Surfaces A 277 (2006) 44–51.
[5] R. Revanur, B. McCloskey, K. Breitenkamp, B.D. Freeman, T. Emrick, Macromolecules 40 (2007) 3624–3630.
[6] W. Xun, H.Y. Wang, Z.Y. Li, S.X. Cheng, X.Z. Zhang, R.X. Zhuo, Colloids and Surfaces B: Biointerfaces 85 (2011) 86–91.
[7] S.D. Xiong, L. Li, J. Jiang, L.P. Tong, S.L. Wu, Z.S. Xu, P.K. Chu, Biomaterials 31 (2010) 2673–2685.
[8] H. Liu, S. Zhang, Y. Li, D. Yang, J. Hu, X. Huang, Polymer 51 (2010) 5198–5206.
[9] Y. Li, S. Zhang, L. Tong, Q. Li, W. Li, G. Lu, H. Liu, X. Huang, Journal of Fluorine Chemistry 130 (2009) 354–360.
[10] J. Mao, P. Ni, Y. Mai, D. Yan, Langmuir 23 (2007) 5127–5134.
[11] M.P. Krafft, Advanced Drug Delivery Reviews 47 (2001) 209–228.
[12] T.M. Massa, W.G. McClung, M.L. Yang, J.Y.C. Ho, J.L. Brash, J.P. Santerre, Journal of Biomedical Materials Research Part A 81 (2007) 178–185.
[13] J.M. Criscione, B.L. Le, E. Stern, M. Brennan, C. Rahner, X. Papademetris, T.M. Fahmy, Biomaterials 30 (2009) 3946–3955.
[14] S.D. Xiong, L. Li, S.L. Wu, Z.S. Xu, P.K. Chu, Journal of Polymer Science, Part A: Polymer Chemistry 47 (2009) 4895–4907.
[15] S. Purser, P.R. Moore, S. Swallow, V. Gouverneur, Chemical Society Reviews 37 (2008) 320–330.
[16] C. Dalvit, A. Vulpetti, ChemMedChem 6 (2011) 104–114.
[17] L. Gu, Z. Shen, C. Feng, Y. Li, G. Lu, X. Huang, G. Wang, J. Huang, Journal of Materials Chemistry 18 (2008) 4332–4340.
[18] T. Takami, Y. Murakami, Colloids and Surfaces B: Biointerfaces 87 (2011) 433–438.
[19] Y. Uchida, Y. Murakami, Colloids and Surfaces B: Biointerfaces 84 (2011) 346–353.
[20] A. Mero, G. Pasut, F.M. Veronese, E. Emilitri, P. Ferruti, Journal of Bioactive and Compatible Polymers 24 (2009) 220–234.
[21] J. Cheng, B.A. Teply, I. Sherifi, J. Sung, G. Luther, F.X. Gu, E.L. Nissenbaum, A.F.R. Moreno, R. Langer, O.C. Farokhzad, Biomaterials 28 (2007) 869–876.
[22] L. Li, Y. Wang, G. Song, S. Wu, P.K. Chu, Z. Xu, Journal of Fluorine Chemistry 130 (2009) 870–877.
[23] Y.B. Song, L.Z. Zhang, W.P. Gan, J.P. Zhu, L.N. Zhang, Colloids and Surfaces B: Biointerfaces 83 (2011) 313–320.
[24] L. Li, Z.S. Xu, G.W. Song, Journal of Fluorine Chemistry 130 (2009) 225–230.
[25] B.S. Kim, J.M. Oh, K.S. Kim, K.S. Seo, J.S. Cho, G. Khang, H.B. Lee, K. Park, M.S. Kim, Biomaterials 30 (2009) 902–909.
[26] T.Y. Liu, S.Y. Chen, D.M. Liu, S.C. Liou, Journal of Controlled Release 107 (2005) 112–121.
[27] Q.H. Zhao, B.Y. Li, Nanomedicine: Nanotechnology, Biology and Medicine 4 (2008) 302–310.
[28] J.H. Kim, Y.H. Bae, European Journal of Pharmaceutical Sciences 23 (2004) 245–251.
[29] L.P. Zhu, Z. Yi, F. Liu, X.Z. Wei, B.K. Zhu, Y.Y. Xu, European Polymer Journal 44 (2008) 1907–1917.
[30] C.T. Lee, C.P. Huang, Y.D. Lee, Biomolecular Engineering 24 (2007) 131–139.
[31] H. Hussain, K. Busse, J. Kressler, Macromolecular Chemistry and Physics 204 (2003) 936–946.
[32] J. Wang, L. Liu, B. Liu, Y. Guo, Y. Zhang, R. Xu, S. Wang, X. Zhang, Spectrochimica Acta, Part A 75 (2010) 366–374.
[33] A. Ravindran, A. Singh, A.M. Raichur, N. Chandrasekaran, A. Mukherjee, Colloids and Surfaces B: Biointerfaces 76 (2010) 32–37.